

Chemical Oxidation of Pyrite by Strong Oxidizing Agents: For Pretreatment of Refractory Pyritic Gold Ores

Abdelkhalek BARBOUCHI^{1,2}, Iman ER-RAQI¹, Rachid IDOUHLI^{1*}, Mohy-Eddine KHADIRI¹, Abdessalem ABOUELFIDA¹, Mehdi LOUARRAT², Mohcine MIKALI^{1,2}, Moulay Abdellah El ALAOUI-CHRIFI², Hakim FAQIR², Intissar BENZAKOUR² and Jaouad BENZAKOUR¹

Authors' affiliations and addresses:

¹ Applied Chemistry and Biomass Laboratory, Department of Chemistry, Cadi Ayyad University, BP 469, 40000 Marrakech, Morocco
e-mail: a.barbouchi.ced@uca.ac.ma

² Reminex Research Center, Managem Group, BP 469, 40000 Marrakech, Morocco
e-mail: a.barbouchi@managemgroup.com

*Correspondence:

Rachid Idouhli, Applied Chemistry and Biomass Laboratory, Department of Chemistry, Cadi Ayyad University, BP 469, 40000 Marrakech, Morocco
tel.: +212 671 78 46 99
e-mail: rachid.idouhli@uca.ac.ma

Acknowledgement:

We thank our sponsors (REMINEX research center, MANAGEM Group, Morocco) who provided insight, expertise and follow-up that greatly assisted this research. The authors are grateful to the Center of Analysis and Characterization (CAC-CIM) at the Cadi Ayyad University, Morocco.

How to cite this article:

Barbouchi, A., Er-raqi, I., Idouhli, R., Khadiri, M.E., Abouelfida, A., Louarrat, M., Mikali, M., El Alaoui-Chrifi, M.A., Faqir, H., Benzakour, I. and Benzakour, J. (2024). Chemical Oxidation of Pyrite by Strong Oxidizing Agents: For Pretreatment of Refractory Pyritic Gold Ores. *Acta Montanistica Slovaca*, Volume 29 (4), 773-786

DOI:

<https://doi.org/10.46544/AMS.v29i4.01>

Abstract

Pyrite is considered the major gold-bearing, in which gold is often finely disseminated throughout the matrix of refractory sulfide ores. To improve the gold extraction, pyrite oxidation is required in order to destroy the refractoriness behavior. This study investigated the use of four oxidizing agents, $S_2O_8^{2-}$, H_2O_2 , ClO_4^- and $Cr_2O_7^{2-}$, to oxidize pyrite. The objective was to enhance the oxidation efficiency of pyrite by optimizing the pH and reaction time conditions. Experimental results showed that the most efficient oxidant for pyrite oxidation was peroxydisulfate $S_2O_8^{2-}$, and the oxidation efficiency of iron in pyrite varies in the following order: $S_2O_8^{2-} > H_2O_2 > ClO_4^- > Cr_2O_7^{2-}$. The optimum pH for the studied oxidizing agents were pH = 6 for $S_2O_8^{2-}$, H_2O_2 , and ClO_4^- , and pH = 2 for $Cr_2O_7^{2-}$, for which the oxidation efficiency reached respectively 76.51%, 20.19%, 16.83%, and 15.40% after 6 hours of reaction. The high oxidation efficiency of pyrite by $S_2O_8^{2-}$ at pH = 6 is explained by the formation of sulfate radical ($SO_4^{\bullet-}$) produced by the activation of $S_2O_8^{2-}$ with Fe^{2+} released from pyrite. The mechanistic insights of the studied oxidizing agents have been elucidated by analyzing the product species after the oxidation reaction in the filtrate by Fourier Transform Infrared (FTIR) spectroscopy and characterizing the solid residue by X-ray diffraction (XRD) and scanning electron microscope (SEM) coupled with energy-dispersive X-ray spectroscopy (EDS). The obtained results suggest that $S_2O_8^{2-}$ is a promising oxidizing agent for the oxidative pretreatment of refractory pyritic gold ores.

Keywords

Refractory gold ores, Pyrite oxidation, Oxidizing agents, Peroxydisulfate



© 2024 by the authors. Submitted for possible open access publication under the terms and conditions of the Creative Commons Attribution (CC BY) license (<http://creativecommons.org/licenses/by/4.0/>).

Introduction

In the last decades, the unsustainable mining of gold has led to the progressive depletion of free-milling gold resources. Consequently, the mining industry has focused its attention on gold ores with complex or refractory character. The term "refractory gold ores" refers to gold ores characterized by a low extraction yield by cyanidation. Therefore, they do not provide economic gold recovery (Fleming, 1992; La Brooy et al., 1994; Rodríguez-Rodríguez et al., 2018; Rogozhnikov et al., 2021).

One of the main causes of the refractoriness behavior is the physical encapsulation of fine particles of gold in sulfide minerals such as pyrite, arsenopyrite, and chalcopyrite (Asamoah et al., 2021; Badri and Zamankhan, 2013; Chryssoulis and McMullen, 2016; Marsden and House, 2006; Pokrovski et al., 2019). Pyrite FeS_2 , also known as iron disulfide, is the most widespread and abundant sulfide mineral on earth (Craig and Vokes, 1993; Forbes et al., 2024; Jefferson et al., 2023; Johnson and Hallberg, 2005; Spietz et al., 2022). It is considered the major gold-bearing, in which gold is often finely disseminated throughout the matrix of refractory sulfide ores.

To destroy the refractoriness behavior and improve gold recovery from refractory pyritic ores, oxidation of pyrite is required to liberate gold. In fact, oxidation is considered a major process for pyrite leaching (Antonijevic et al., 1997). Moreover, pyrite oxidation is an electrochemical process involving electron transfer between iron and/or sulfur, constituting pyrite and the reagent used as an oxidant (Holmes and Crundwell, 2000).

Pyrite is classified as the most noble and inert sulfide mineral with a rest potential of 0.66 V/SHE (Tab. 1) (Chandra and Gerson, 2010). This electrochemical behavior of pyrite requires the use of oxidizing agents with high oxidation-reduction potential to make the oxidation possible thermodynamically. Theoretically, a higher value of E° signifies that the oxidant becomes stronger (Fig. 1). However, using these oxidants for pyrite oxidation requires an optimization of conditions to enhance the oxidation efficiency.

Tab. 1. Rest potential of some sulfide minerals measured under standard conditions (Chandra and Gerson, 2010)

Sulfide mineral	Rest potential (V/SHE)
Pyrite	0.66
Chalcopyrite	0.56
Sphalerite	0.46
Covellite	0.45
Bornite	0.42
Galena	0.40

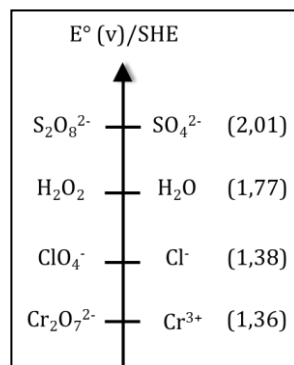
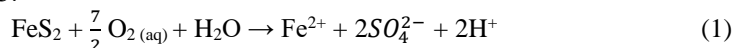


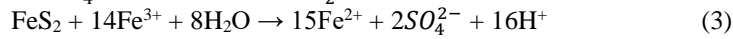
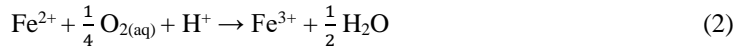
Fig. 1. Standard potential of the studied oxidizing agents (Barbouchi et al., 2024)

The oxidation of pyrite is known as a complex process due to the involvement of many elementary routes of iron and sulfur in the mechanism (Dos Santos et al., 2016). According to Ahlberg et al. (1990), two main mechanisms have been suggested to describe the oxidation of pyrite:

1. Preferential oxidation of sulfur atoms in pyrite to sulfate or another form, which the oxidation of pyrite started first with the release of sulfur to sulfate, and then hydroxide ions react with iron in the surface sites to form an iron hydroxide.
2. Preferential release of iron atoms into solution or into precipitated form as hydroxide, which the mechanism carries out via progressive release on metal sites, leaving sulfur atoms unreacted.

Chandra et al. cited studies by several researchers who worked on the aqueous oxidation of pyrite by O_2 or Fe^{3+} , and they suggest that the pyrite oxidation may involve both oxidation of iron from Fe^{2+} to Fe^{3+} and sulfur from S_2^{2-} to SO_4^{2-} (Chandra and Gerson, 2010). The overall mechanism reported by these authors is shown in Eqs. 1–3:





Recent studies have shown that the types of products formed during pyrite oxidation are influenced by the oxidant used and the pH of the solution (Huang et al., 2023; Tu et al., 2017; Xu et al., 2022). Feng et al. reported that in aqueous media, intermediate products such as elemental sulfur (S_0), thiosulfate ($\text{S}_2\text{O}_3^{2-}$), hydrogen sulfide (H_2S), and polysulfides can form, eventually converting to sulfate ions (SO_4^{2-}) (Feng et al. 2019). Liu et al. identified additional sulfur species during pyrite oxidation, including sulfite (SO_3^{2-}), trithionate ($\text{S}_3\text{O}_6^{2-}$), tetrathionate ($\text{S}_4\text{O}_6^{2-}$), and pentathionate ($\text{S}_5\text{O}_6^{2-}$) (Liu et al. 2023). Li et al. revealed that during microbial oxidation of pyrite, the sulfur oxidation sequence progresses from sulfide (S^{2-}) and bisulfide (S_2^-) to intermediate polysulfides (S_n^{2-}), then to elemental sulfur (S_0), followed by sulfite (SO_3^{2-}), and to thiosulfate ($\text{S}_2\text{O}_3^{2-}$), which is further oxidized to sulfate (SO_4^{2-}) (Li et al. 2016).

This paper aims to investigate the oxidation efficiency of pyrite by $\text{S}_2\text{O}_8^{2-}$, H_2O_2 , ClO_4^- and $\text{Cr}_2\text{O}_7^{2-}$ oxidizing agents. The parameters studied were pH and reaction time. The mechanistic aspects of the studied oxidizing agents have been discussed by analyzing the product species in the filtrate by Fourier Transform Infrared (FTIR) spectroscopy and characterizing the solid residue after the oxidation reaction by X-ray diffraction (XRD) and scanning electron microscope (SEM) coupled with energy-dispersive X-ray spectroscopy (EDS).

Materials and Methods

Mineral sample

The experiments were carried out on a high-purity pyrite crystal specimen (not refractory gold ore) to eliminate interference of other compounds). The pyrite mineral was obtained from the Oumjrane Mine of Managem Group (Eastern Anti-Atlas, Morocco). The sample was characterized using X-ray diffraction with an AERIS Panalytical diffractometer (Cobalt, $\text{K}\alpha$ radiation; $\lambda = 1.724 \text{ \AA}$), equipped with HighScore Plus software for mineralogical identification. The chemical composition was analyzed using atomic absorption spectroscopy (AAS) with the Agilent 280 FS Flame technique for iron analysis and inductively coupled plasma atomic emission spectroscopy (ICP-AES) with the Agilent 5110 SVDV for sulfur analysis. The sample has been ground using a mortar mill to the particle size distribution of $D_{80} = 75 \mu\text{m}$.

Chemical reagents

The oxidizing agents investigated in this study are potassium peroxydisulfate $\text{K}_2\text{S}_2\text{O}_8$, hydrogen peroxide H_2O_2 , sodium perchlorate NaClO_4 and potassium dichromate $\text{K}_2\text{Cr}_2\text{O}_7$. Sulfuric acid H_2SO_4 and sodium hydroxide NaOH were used to adjust the pH of the solution. All reagents were analytical-grade products.

Experimental procedure

The experiments were carried out in a glass beaker of 400 mL. The beaker was filled with 250 mL of the solution containing 0.1 M of the oxidant and adjusted to the desired pH value (with monitoring).

The solution was stirred with a magnetic stirrer at a speed of 400 rpm. All the experiments were conducted at 25 °C. As soon as the solution is prepared, 0.5g of pyrite powder is added, and the oxidative reaction is then started. The fraction of pyrite reacted over time was determined by taking 7 samples of the filtered suspensions at 30min, 1h, 1h30min, 2h, 4h, 6h, and 24h. Iron content in these samples was analyzed by atomic absorption spectroscopy AAS. The experiments were conducted in duplicate, and the values presented are the average of the two trials. The oxidation efficiency of iron in pyrite was calculated according to (Eq. 4):

$$\text{Oxidation efficiency of iron in pyrite (\%)} \quad \alpha = \frac{C_{\text{TFe}} \times V \times M(\text{FeS}_2)}{m \times M(\text{Fe})} \times 100 \quad (4)$$

Where:

C_{TFe} is the total iron concentration measured in the solution (g/L), V is the volume of the solution (L), $M(\text{FeS}_2)$ is the molecular mass of pyrite (g/mol), m is the mass of pyrite (g), and $M(\text{Fe})$ is the molecular mass of iron (g/mol).

After a residence time of 24h, the solution was filtered, and the solid residue was washed with distilled water and dried for subsequent characterization. Scanning electron microscopy (SEM) combined with energy-dispersive X-ray (EDX) microanalysis was used to examine pyrite particles' morphology and chemical composition after the oxidation process using a TESCAN VEGA3 SEM electron microscope. The filtrate was analyzed by FTIR spectroscopy to identify functional groups and their associated vibration modes using a VERTEX 70 FT-IR Spectrometer equipped with an attenuated total reflection (ATR) accessory. The sulfate content was determined gravimetrically as BaSO_4 by UV-visible spectrophotometry using a Shimadzu UV-3600 spectrophotometer equipped with an integrating sphere.

Results and discussion

Sample characterization

Mineralogical characterization by XRD of the sample showed that the only existing phase is pyrite (Fig. 2). This was confirmed by chemical analysis of the sample with AAS and ICP-AES, which showed respectively an element composition of Fe 45.81 wt. % and S 52.63 wt. %, compared to Fe 46.55 wt.% and S 53.45 wt.% for stoichiometric FeS_2 .

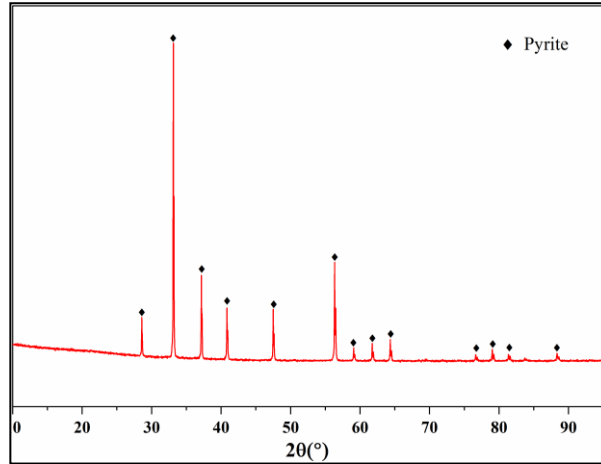


Fig. 2. XRD pattern of the pyrite crystal specimen

Oxidation by $\text{S}_2\text{O}_8^{2-}$

The experiments of pyrite oxidation by $\text{S}_2\text{O}_8^{2-}$ were carried out over a wide range of pH values from 2 to 12. The oxidation efficiency of pyrite is illustrated in Fig. 3. It can be shown from the oxidation curves that the oxidation rate was highest at pH 6 and decreased with either an increase or a decrease in pH within the range of pHs examined in this study. At pH = 6, the oxidation reaches a plateau by achieving 76.51% after a residence time of 6 hours, which was the maximum rate registered in all the studied pH values. However, it is clear that the oxidation in an acidic medium (pHs 2 and 4) was lower than in an alkaline medium (pHs 8, 10, and 12). After 24 hours of reaction, the oxidation rate achieved 22.14% and 32% at pH 2 and 4, respectively, and reached 45.28%, 37.10%, and 42.81%, respectively, at pH 8, 10, and 12.

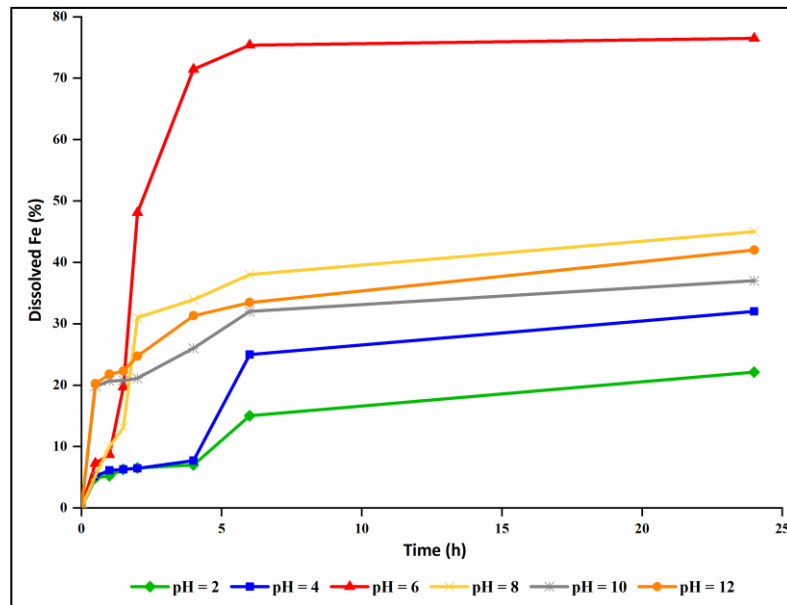
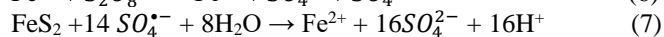
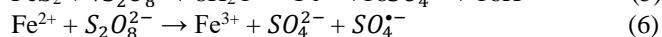
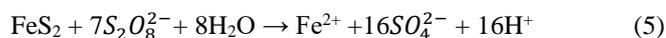


Fig. 3. Effect of pH on the oxidation efficiency of pyrite by $\text{S}_2\text{O}_8^{2-}$. $[\text{Ox}] = 0.1 \text{ M}$

The high oxidation efficiency of pyrite at pH = 6 could be explained by the formation of sulfate radical ($\text{SO}_4^{\bullet-}$) produced by the activation of $\text{S}_2\text{O}_8^{2-}$ with Fe^{2+} released from pyrite. Sulfate radical ($\text{SO}_4^{\bullet-}$) is known as a strong one-electron oxidizing agent with highly oxidative potential ($E^\circ = 2.6 \text{ V vs. NHE}$) (Duan et al., 2022; Li et

al., 2022; Xie et al., 2023), and several investigations have proved that $S_2O_8^{2-}$ can be activated by Fe^{2+} , leading to the generation of $SO_4^{\bullet-}$ (Karim et al., 2021; Matzek and Carter, 2016; Xie et al., 2023). The oxidation of pyrite by $S_2O_8^{2-}$ leads to the production of Fe^{2+} ions, according to (Eq. 5) (Gui et al., 2023). Fe^{2+} activates $S_2O_8^{2-}$ and favors the formation of sulfate radicals $SO_4^{\bullet-}$ (Eq. 6). Consequently, the oxidation efficiency is enhanced by further oxidation of pyrite by the sulfate radicals formed (Eq. 7).



In addition, it can be seen from (Fig. 3) that the oxidation rate under alkaline conditions ($pH \geq 8$) was higher than in acidic conditions ($pH \leq 4$). This could be explained by the formation of hydroxyl radicals in alkaline pH, as reported by Hao et al. (2014). At $pH \geq 8$, sulfate radicals may react with OH^- by radical interconversion reactions to produce hydroxyl radicals according to (Eq. 8) (Ahmadi et al., 2016; Furman et al., 2010):



Hydroxyl radicals HO^{\bullet} are also characterized by strong oxidative potential ($E = 2.8$ V vs NHE) (Duan et al., 2022; Li et al., 2022), which seem capable of oxidizing pyrite theoretically. However, according to Luo et al. and Araújo et al., hydroxyl radicals have a shorter lifetime and smaller performance for electron transfer reactions compared to sulfate radicals (Araújo et al., 2022; Luo et al., 2016). Therefore, in alkaline pH, OH^- ions act as scavengers of sulfate radicals and then decrease pyrite's oxidation reaction. Similar results have been reported for oxidation by persulfate in alkaline pH of ammonium perfluorooctanoate (Hao et al., 2014) and trichloroethylene (Liang et al., 2007).

The analysis of sulfate concentration by UV-Vis spectrophotometry in the filtrate after a residence time of 24h for all pHs evaluated in this study is given in (Fig. 4) and shows that the higher sulfate concentration is registered at pHs 2 and 4. Therefore, it can be concluded that the lowest oxidation rates of pyrite registered at acidic conditions ($pH \leq 4$) could be attributed to the decomposition of $S_2O_8^{2-}$ to SO_4^{2-} without generation of sulfate radicals. These results are in agreement with those found by Liang et al., which indicate that sulfate may inhibit the reactivity of sulfate radicals (Liang et al., 2007). However, House et al. reported that acidic conditions are more favorable for $SO_4^{\bullet-}$ formation due to acid catalyzation (House, 1962). Nevertheless, Peyton et al. revealed that a higher sulfate radical concentration may favor the $SO_4^{\bullet-}/SO_4^{\bullet-}$ (Eq. 9) or $SO_4^{\bullet-}/S_2O_8^{2-}$ (Eq. 10) reactions (Peyton, 1993). Consequently, when more sulfate radical is formed (e.g., via acidic activation), there will be scavenging of $SO_4^{\bullet-}$ by itself and compete with $SO_4^{\bullet-}$ /pyrite interaction.

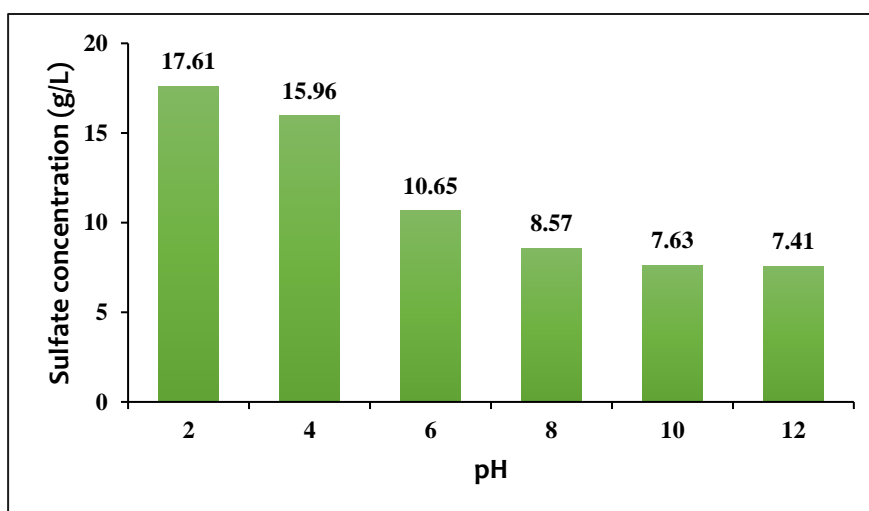
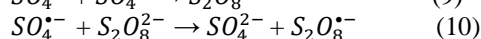
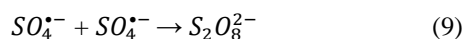


Fig. 4. Sulfate concentration in the solution after 24h of reaction

Oxidation with H_2O_2

The oxidation tests of pyrite by H_2O_2 have been examined in a pH range varying from 2 to 12. The obtained results (Fig. 5) showed that the oxidation of pyrite by H_2O_2 is favored only at $pH \leq 6$ and dropped in alkaline medium at $pH \geq 8$. The oxidation rate for pHs 2, 4, and 6 reached 19.08%, 19.93%, and 20.19%, respectively, after

a residence time of 6 hours. In addition, it can be seen from the figure that the reaction rate increases slightly after 6 hours of the reaction, and the oxidation efficiency achieved 19.17%, 20.87%, and 21.71% for pHs 2, 4, and 6, respectively. However, for pHs 8, 10, and 12, the oxidation rate does not exceed 1% even after 24 hours of reaction.

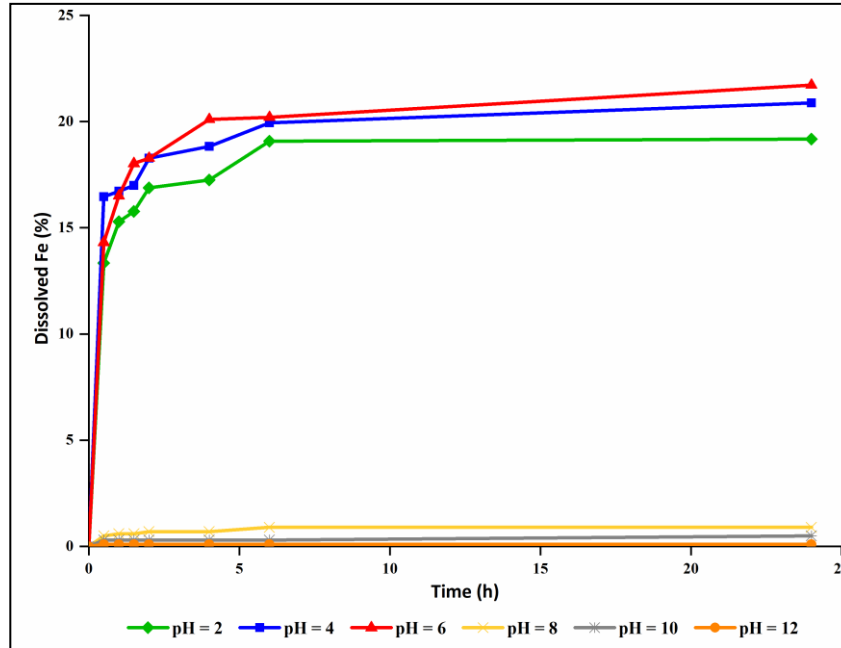
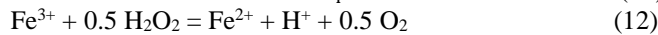
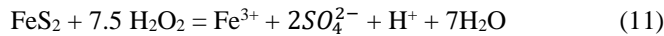


Fig. 5. Effect of pH on the oxidation efficiency of pyrite by H_2O_2 . $[Ox] = 0.1 M$

It can be concluded that the oxidation of pyrite by H_2O_2 is inefficient in alkaline pH compared to acidic pH. According to Irum et al., OH^- ions in alkaline pH ($pH \geq 8$) react with Fe^{2+} to form $Fe(OH)_2$ as a gelatinous substance, which inhibits the oxidation of pyrite via its adherence on the surface (Irum et al., 2017). Therefore, low oxidation rates of pyrite have been obtained in this pH range. In addition, even in acidic media ($pH \leq 6$), low oxidation rates of pyrite have been achieved. This could be attributed to the catalytic decomposition of H_2O_2 in the presence of pyrite. Based on investigations conducted by several authors, the overall reaction of pyrite oxidation by H_2O_2 in acidic pH can be demonstrated by (Eq. 11), and the ferric iron produced can act as a catalyst of H_2O_2 decomposition according to (Eq. 12) (Chirita, 2009; Iraola-Arregui et al., 2018; Karppinen et al., 2024; Marzacco, 1999; Nicol, 2020; Petrović et al., 2023; Salas-Martell et al., 2020; Tehrani et al., 2021). Also, it was shown that the decomposition of H_2O_2 could be catalyzed via heterogeneous reaction by iron sites present on the surface of pyrite, resulting in a significant loss of reagent (Chirita, 2009; Petrović et al., 2023; Nicol, 2020).



Other investigations suggest that the released oxygen from H_2O_2 decomposition in (Eq. 12) may adsorb on the pyrite surface and inhibit the reaction between pyrite and H_2O_2 , thereby decreasing the oxidation rate (Antonić et al., 1997; Dimitrijević et al., 1999; Hao et al., 2022).

Oxidation with ClO_4^-

The oxidation experiments of pyrite oxidation by ClO_4^- , were conducted in acidic and alkaline mediums from pH 2 to 12. The results are given in (Fig. 6), and show that oxidation of pyrite by ClO_4^- is more favored at $pH \leq 6$ and decreases by increasing pH from 8 to 12. Moreover, it can be seen that the oxidation curves for pH 2, 4, and 6 have almost the same behavior, and the oxidation rate achieved respectively 22.03%, 21.71%, and 23.18% after 24 hours of reaction.

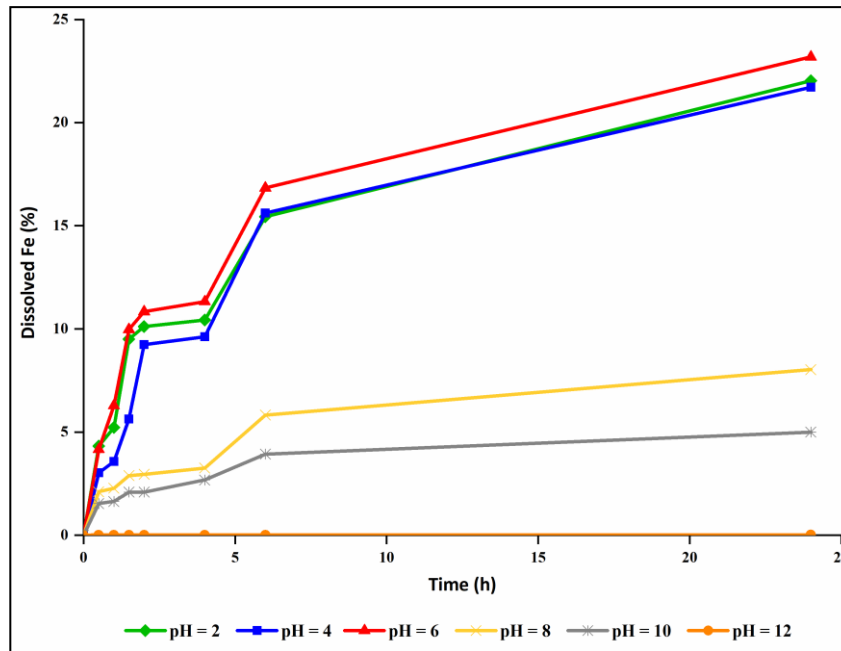
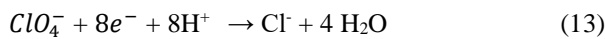


Fig. 6. Effect of pH on the oxidation efficiency of pyrite by ClO_4^- . $[Ox] = 0.1 M$

The reduction of perchlorate involves the transfer of eight electrons (Eq. 13), which results in a high standard potential ($E^\circ = 1.388 V$).



Despite that, the oxidation of pyrite by this oxidant did not show a significant efficiency. This could be attributed to the stability of perchlorate. According to the E-pH diagram of the chlorine-water system (Fig. 7), ClO_4^- is stable in all the pH ranges, and it can be seen that the potential decreases by increasing the pH value, indicating that the oxidation seems to be more efficient in acidic media.

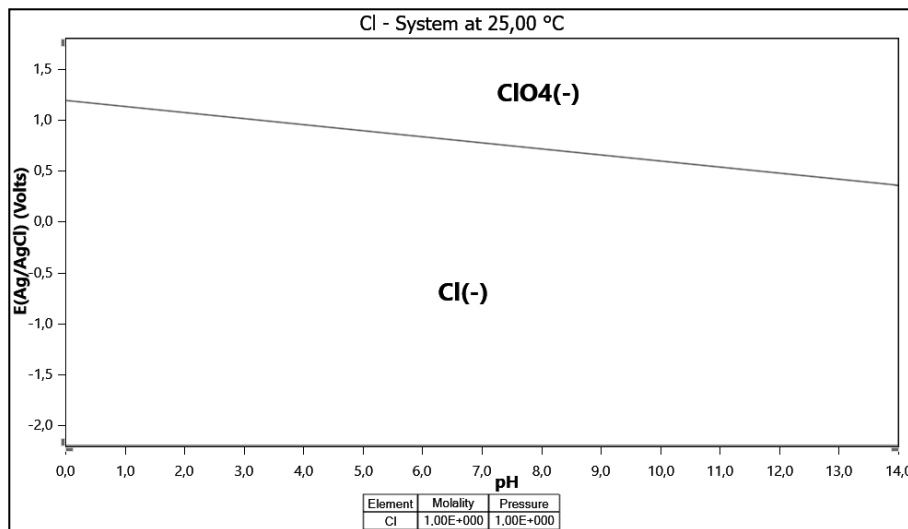


Fig. 7. Potential-pH equilibrium diagram of the system chlorine-water. Constructed by HSC Chemistry 10.2.2.0 software

In addition, according to Urbansky et al., perchlorate reduction is characterized by slow kinetics and can occur only in the presence of highly concentrated acid, which agrees with our findings of pyrite oxidation in alkaline pH. Also, it has been mentioned that even in the range of acid concentration 0.1 to 4.0 M, perchlorate is not reduced by ferrous iron (Fe^{2+}), which could be released from pyrite (Levakov et al., 2021; Mitra et al., 2020; Urbansky, 2002).

Oxidation with $Cr_2O_7^{2-}$

The effect of pH on pyrite oxidation by $Cr_2O_7^{2-}$ was investigated at pH values 2, 4, and 6 since this oxidant is stable only in this pH range according to the potential-pH equilibrium diagram of the system chromium-water (Pourbaix, 1974). The results obtained (Fig. 8) show that the oxidation occurs only at pH = 2, while at pHs 4 and 6, the oxidation rate does not exceed 1%. On the other hand, even at pH 2, the oxidation achieves only 15.40% after 6 hours and increases slightly to 17.36 after 24 hours of reaction.

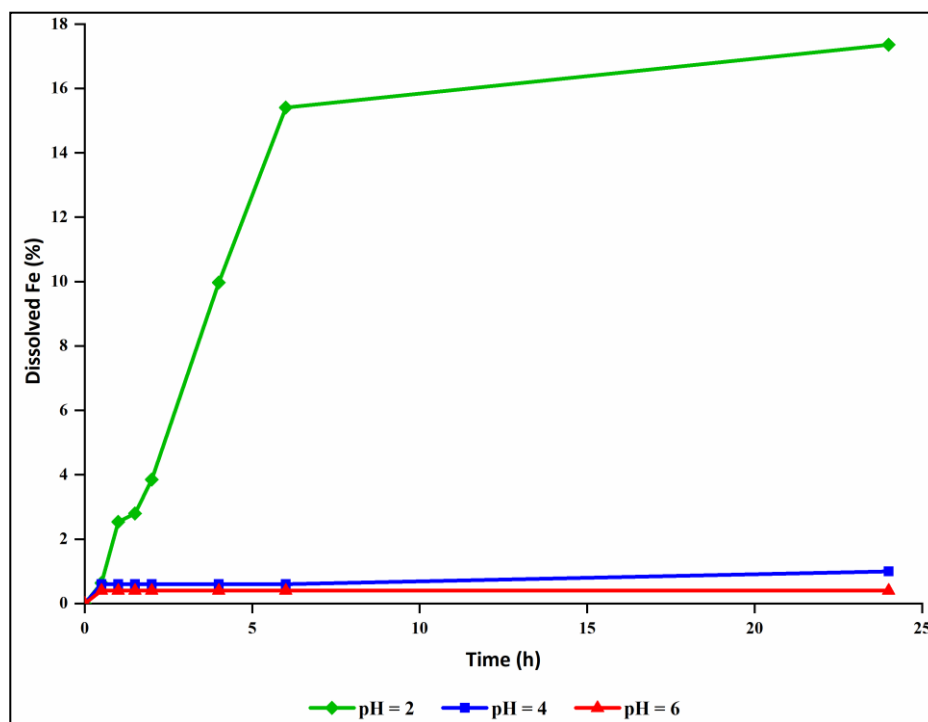
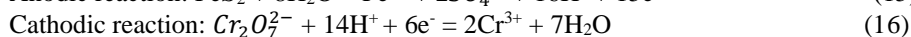
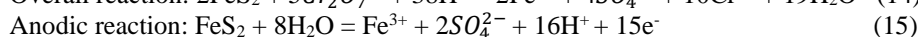
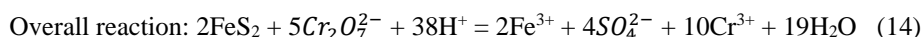


Fig. 8. Effect of pH on the oxidation efficiency of pyrite by $Cr_2O_7^{2-}$. $[Ox] = 0.1 M$

The electrochemical reaction of pyrite oxidation by $Cr_2O_7^{2-}$ can be established as given in (Eq. 14), which can be split into two electrochemical half-reactions: the anodic half-reaction (Eq. 15) and the cathodic half-reaction (Eq. 16).



However, the low oxidation rate obtained in pyrite oxidation by $Cr_2O_7^{2-}$ could be attributed to the chemisorption of chromium (VI) on the pyrite surface (Chen et al., 2021; Zhang et al., 2022). According to findings by Antonijevic et al., chromium (VI) present in $Cr_2O_7^{2-}$ can probably saturate the surface of pyrite and then inhibit the galvanic interaction between $Cr_2O_7^{2-}$ and pyrite (Antonijevic et al., 1993). In addition, it can be concluded that pH = 2 is the optimum condition for pyrite oxidation by $Cr_2O_7^{2-}$ in the range of pHs evaluated in this study. This is due to the catalytic role of H^+ ions, which positively affect the oxidation rate of pyrite (Antonijevic et al., 1993). Similar results were obtained by Chirita, showing that pyrite oxidation increases with the increase in solution acidity (Chirita, 2003).

Comparison and mechanistic insights of oxidizing agents

By comparing the oxidation efficiency of pyrite by the studied oxidizing agents under their optimum condition of pH ($S_2O_8^{2-}$ at pH 6, H_2O_2 at pH 6, ClO_4^- at pH 6 and $Cr_2O_7^{2-}$ at pH 2) (Fig. 9), it was found that $S_2O_8^{2-}$ is the most efficient oxidant for Fe pyrite oxidation.

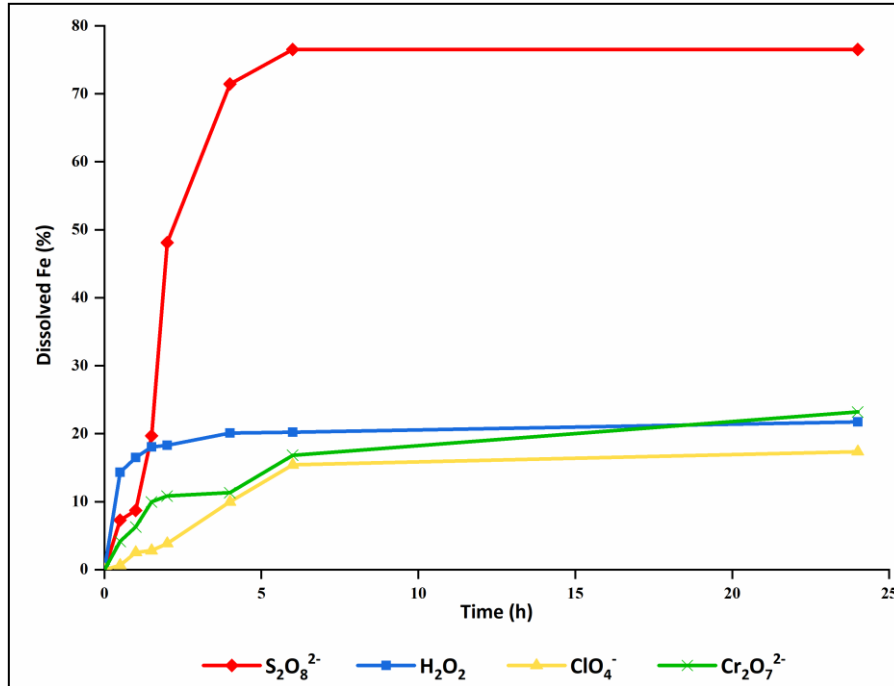


Fig. 9. Comparison of the oxidation efficiency of pyrite by the studied oxidants. [Ox] = 0.1 M

The solid residues of pyrite after oxidation for the four oxidants under their optimum condition of pH have been characterized by XRD (Fig. 10) and by SEM-EDS (Fig. 11). The result of XRD showed that the pyrite remains unchanged, and there is no formation of new phases or compounds after the oxidation process.

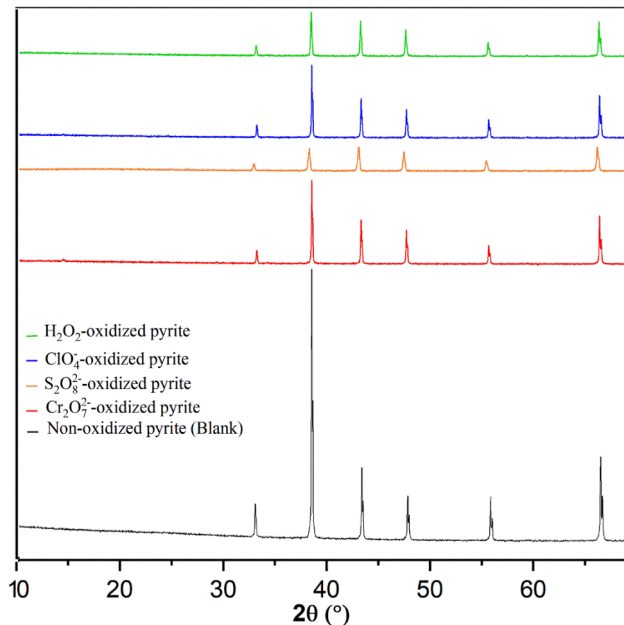


Fig. 10. XRD pattern of pyrite residues after the oxidation process

Zhong et al. demonstrated through XRD and XPS analysis that elemental sulfur S^0 is formed when pyrite is oxidized by ferric iron Fe^{3+} (Zhong, 2015). However, according to Flatt et al. and Miller et al., the elemental sulfur S^0 is known as cyanide consuming agent and can inhibit gold cyanidation by overconsumption of cyanide to form thiocyanate (Eq. 17) (Flatt and Woods, 1995; Miller and Brown, 2016).



Therefore, the studied oxidizing agents, especially $S_2O_8^{2-}$, do not adversely affect the cyanidation process when used in the pretreatment of refractory gold ores, as elemental sulfur is not produced after oxidation.

Moreover, SEM characterization coupled with energy-dispersive X-ray spectroscopy (EDS) showed a reduction in pyrite particle size in all pyrite residues (Fig. 11). SEM micrographs also showed the presence of micro-cracks in the pyrite after the oxidation with $S_2O_8^{2-}$ and H_2O_2 due to the aggressive attack of these oxidants. In addition, an analysis of elemental composition using the EDS technique for all pyrite residues in different spots revealed the presence of oxygen, demonstrating the formation of oxide particles that seem to be iron oxides.

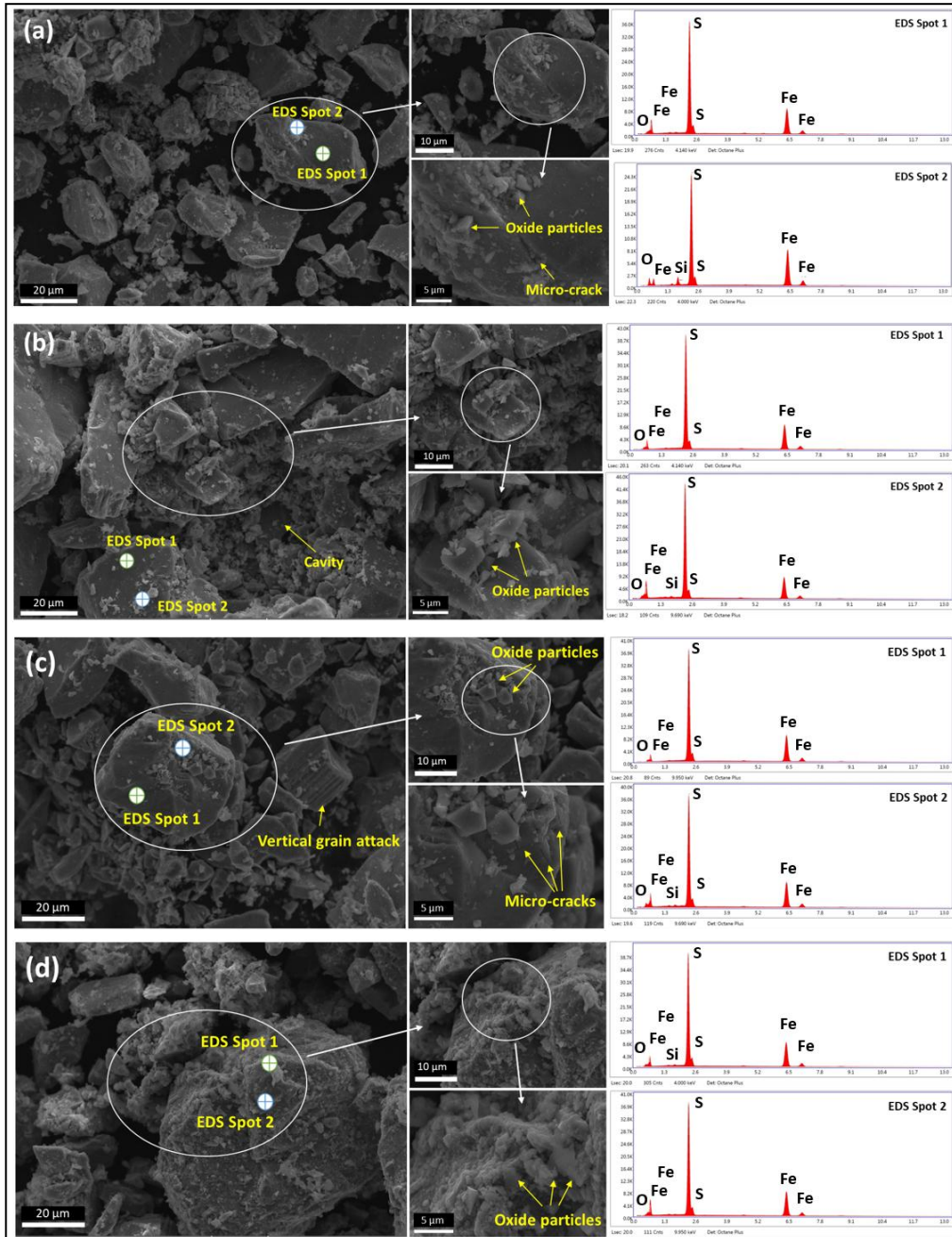


Fig. 11. SEM images and the corresponding EDS spectrum of pyrite after the oxidation process. (a) H_2O_2 -oxidized pyrite, (b) $Cr_2O_7^{2-}$ -oxidized pyrite, (c) $S_2O_8^{2-}$ -oxidized pyrite, and (d) ClO_4^- -oxidized pyrite

On the other hand, the products formed in the solution have been identified by analyzing the chemical bonds using FTIR spectroscopy. (Fig. 12) shows FTIR spectra of the solution filtrate after the oxidation of pyrite for the studied oxidants under their optimum pH condition. The band at 610 cm^{-1} corresponds to SO_4^{2-} (Das et al., 2014; Radha et al., 2015), which shows the oxidation of S_2^{2-} in pyrite to sulfate. The sulfate formed could attached to iron and form Fe- SO_4 according to the band located at 1625 cm^{-1} (Khataee et al., 2016). However, this band is

strong in H_2O_2 filtrate and weak in $S_2O_8^{2-}$, $Cr_2O_7^{2-}$ and ClO_4^- filtrates. The band at 1230 cm^{-1} appears only in $S_2O_8^{2-}$ filtrate, which is attributed to the S–O stretching of sulfate species (Caldeira et al., 2003). In addition, the transmission bands at 870 cm^{-1} and 1090 cm^{-1} correspond to Fe–O and Fe–OH, respectively (Corrêa et al., 2016; Yadav et al., 2020). This suggests that pyrite is oxidized and transformed into iron oxide and iron hydroxide. Furthermore, it can be seen as a broad band at 3450 cm^{-1} , which is attributed to the stretching modes of the water molecules (Khataee et al., 2016). This band is large in H_2O_2 filtrate because of the O–H bonds of this oxidant.

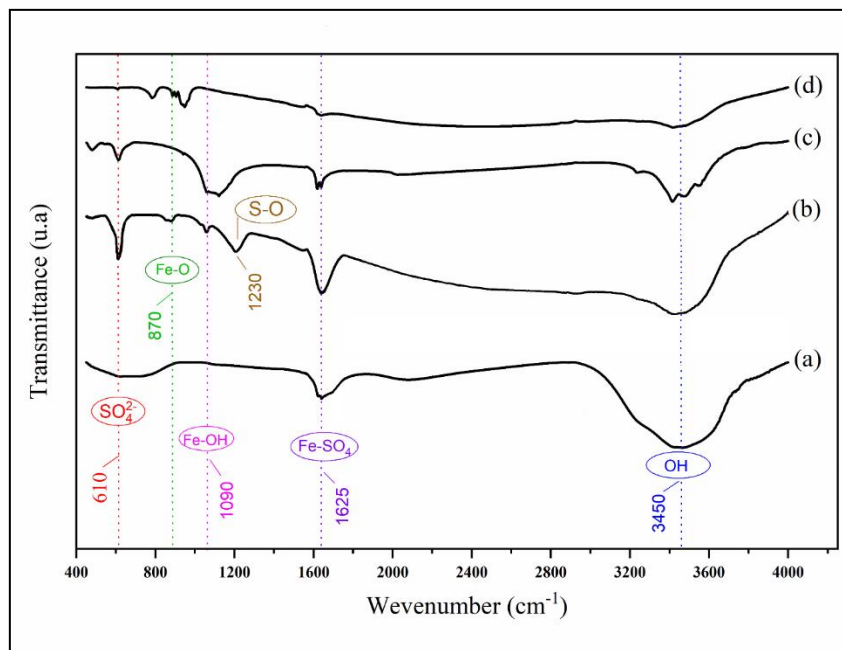


Fig. 12. FTIR spectra of the solution filtrate: (a) H_2O_2 filtrate, (b) $S_2O_8^{2-}$ filtrate, (c) ClO_4^- filtrate, and (d) $Cr_2O_7^{2-}$ filtrate

Conclusions

The extraction of gold from refractory ores poses significant challenges due to the encapsulation of gold within sulfide minerals, mainly pyrite. This study proposes an effective solution for pyrite oxidation to address this issue. Four oxidizing agents have been investigated for the oxidation of a high-purity pyrite crystal specimen. The most efficient oxidant for pyrite oxidation was $S_2O_8^{2-}$, and the oxidation efficiency of iron in pyrite varies in the following order: $S_2O_8^{2-} > H_2O_2 > ClO_4^- > Cr_2O_7^{2-}$. The optimum condition of pH for the studied oxidizing agent were pH = 6 for $S_2O_8^{2-}$, pH ≤ 6 for H_2O_2 , pH ≤ 6 for ClO_4^- , and pH = 2 for $Cr_2O_7^{2-}$, which the oxidation efficiency reached respectively 76.51%, [19.08%; 20.19%], [15.44%; 16.83%], and 15.40% after 6 hours of reaction. The high oxidation efficiency of pyrite by $S_2O_8^{2-}$ at pH = 6 is explained by the formation of sulfate radicals ($SO_4^{\bullet-}$) produced by the activation of $S_2O_8^{2-}$ with Fe^{2+} released from pyrite. Characterization by XRD of the solid residues of pyrite after oxidation showed that the pyrite remains unchanged and no new phases or compounds are formed. SEM-EDS also showed that the size of particles has been reduced and revealed the formation of oxide particles that seem to be iron oxides. This study will contribute to developing new oxidative pretreatment processes using persulfate for refractory pyritic gold ores.

References

- Ahlberg, E., Forssberg, K.S.E. & Wang, X. The surface oxidation of pyrite in alkaline solution. *J Appl Electrochem* 20, 1033–1039 (1990). <https://doi.org/10.1007/BF01019585>
- Ahmadi, M., Behin, J., Mahnam, A.R., (2016). Kinetics and thermodynamics of peroxydisulfate oxidation of Reactive Yellow 84. *Journal of Saudi Chemical Society* 20, 644–650. <https://doi.org/10.1016/j.jscs.2013.07.004>
- Antonijević, M., Dimitrijević, M., & Janković, Z. (1997). Leaching of pyrite with hydrogen peroxide in sulphuric acid. *Hydrometallurgy*, 46(1-2), 71-83. [https://doi.org/10.1016/S0304-386X\(96\)00096-5](https://doi.org/10.1016/S0304-386X(96)00096-5)
- Antonijević, M., Dimitrijević, M., & Janković, Z. (1993). Investigation of pyrite oxidation by potassium dichromate. *Hydrometallurgy*, 32(1), 61-72. [https://doi.org/10.1016/0304-386X\(93\)90056-J](https://doi.org/10.1016/0304-386X(93)90056-J)

- Araújo, K.C., dos Santos, E. V., Nidheesh, P. V., Martínez-Huitle, C.A., (2022). Fundamentals and advances on the mechanisms of electrochemical generation of persulfate and sulfate radicals in aqueous medium. *Curr Opin Chem Eng* 38. <https://doi.org/10.1016/j.coche.2022.100870>
- Asamoah, R. K., Zanin, M., Skinner, W., & Addai-Mensah, J. (2021). Refractory gold ores and concentrates part 2: gold mineralisation and deportment in flotation concentrates and bio-oxidised products. *Mineral Processing and Extractive Metallurgy: Transactions of the Institute of Mining and Metallurgy*, 130(4), 269–282. <https://doi.org/10.1080/25726641.2019.1626660>
- Badri, R., Zamankhan, P., (2013). Sulphidic refractory gold ore pretreatment by selective and bulk flotation methods. *Advanced Powder Technology* 24, 512–519. <https://doi.org/10.1016/j.appt.2012.10.002>
- Barbouchi, A., Er-raqi, I., Hamchi, M., Idouhli, R., Khadiri, M., Abouelfida, A., El Alaoui-Chrifi, M.A., Faqir, H., Benzakour, I., Benzakour, J., 2024. Chemical oxidation of arsenopyrite by strong oxidizing agents: For oxidative pretreatment of refractory arsenopyritic gold ores. *Acta Geodynamica et Geomaterialia* 185–194. <https://doi.org/10.13168/AGG.2024.0017>
- Caldeira, C.L., Ciminelli, V.S.T., Dias, A., Osseo-Asare, K., (2003). Pyrite oxidation in alkaline solutions: Nature of the product layer. *Int J Miner Process* 72, 373–386. [https://doi.org/10.1016/S0301-7516\(03\)00112-1](https://doi.org/10.1016/S0301-7516(03)00112-1)
- Chandra, A.P., Gerson, A.R., (2010). The mechanisms of pyrite oxidation and leaching: A fundamental perspective. *Surf Sci Rep* 65, 293–315. <https://doi.org/10.1016/j.surfrep.2010.08.003>
- Chen, Y., Gan, M., He, P., Zhang, K., Wang, X., Zhu, J., Liu, M., Chen, F., Zhu, J., & Xiao, N. (2021). Efficient removal of Cr(VI) from aqueous solution by natural pyrite/rhodochrosite derived materials: Performance, kinetic and mechanism. *Advanced Powder Technology*, 32(10), 3814–3825. <https://doi.org/10.1016/j.appt.2021.08.032>
- Chirita, P., (2009). Hydrogen Peroxide Decomposition by Pyrite in the Presence of Fe(III)-ligands. *Chem Biochem Eng Q* 23, 259–265.
- Chirita, P., (2003). Kinetics of Aqueous Pyrite Oxidation by Potassium Dichromate - An Experimental Study. *Turk J Chem* 27, 111–118.
- Chrysosoulis, S.L., McMullen, J., (2016). Mineralogical Investigation of Gold Ores, in: *Gold Ore Processing: Project Development and Operations*. Elsevier, pp. 57–93. <https://doi.org/10.1016/B978-0-444-63658-4.00005-0>
- Corrêa, S., Lacerda, L.C.T., Pires, M.D.S., Rocha, M.V.J., Nogueira, F.G.E., Da Silva, A.C., Pereira, M.C., De Brito, A.D.B., Da Cunha, E.F.F., Ramalho, T.C., (2016). Synthesis, Structural Characterization, and Thermal Properties of the Poly(methylmethacrylate)/ δ -FeOOH Hybrid Material: An Experimental and Theoretical Study. *J Nanomater* 2016. <https://doi.org/10.1155/2016/2462135>
- Craig, J.R., Vokes, F.M., (1993). The metamorphism of pyrite and pyritic ores: an overview. *Mineral Mag* 57, 3–18.
- Das, G., Kakati, N., Lee, S.H., Karak, N., Yoon, Y.S., (2014). Water soluble sodium sulfate nanorods as a versatile template for the designing of copper sulfide nanotubes. *J Nanosci Nanotechnol* 14, 4455–4461. <https://doi.org/10.1166/jnn.2014.8282>
- Dimitrijević, M., Antonijević, M., & Dimitrijević, V. (1999). Investigation of the kinetics of pyrite oxidation by hydrogen peroxide in hydrochloric acid solutions. *Minerals Engineering*, 12(2), 165-174. [https://doi.org/10.1016/S0892-6875\(98\)00129-0](https://doi.org/10.1016/S0892-6875(98)00129-0)
- Dos Santos, E.C., De Mendonça Silva, J.C., Duarte, H.A., (2016). Pyrite Oxidation Mechanism by Oxygen in Aqueous Medium. *Journal of Physical Chemistry C* 120, 2760–2768. <https://doi.org/10.1021/acs.jpcc.5b10949>
- Duan, X., Niu, X., Gao, J., Waclawek, S., Tang, L., Dionysiou, D.D., (2022). Comparison of sulfate radical with other reactive species. *Curr Opin Chem Eng*. <https://doi.org/10.1016/j.coche.2022.100867>
- Feng, J., Tian, H., Huang, Y., Ding, Z., & Yin, Z. (2019). Pyrite oxidation mechanism in aqueous medium. In *Journal of the Chinese Chemical Society* (Vol. 66, Issue 4, pp. 345–354). Chinese Chemical Society Taiwan. <https://doi.org/10.1002/jccs.201800368>
- Flatt, J.R., Woods, R. A voltammetric investigation of the oxidation of pyrite in nitric acid solutions: relation to treatment of refractory gold ores. *J Appl Electrochem* 25, 852–856 (1995). <https://doi.org/10.1007/BF00772204>
- Fleming, C. (1992). Hydrometallurgy of precious metals recovery. *Hydrometallurgy*, 30(1-3), 127-162. [https://doi.org/10.1016/0304-386X\(92\)90081-A](https://doi.org/10.1016/0304-386X(92)90081-A)
- Forbes, E., Jefferson, M., Yenial-Arslan, U., Curtis-Morar, C., & O'Donnell, R. (2024). Solving the mystery of natural pyrite flotation – A mineralogy-based approach. *Minerals Engineering*, 207. <https://doi.org/10.1016/j.mineng.2023.108544>
- Furman, O.S., Teel, A.L., Watts, R.J., (2010). Mechanism of base activation of persulfate. *Environ Sci Technol* 44, 6423–6428. <https://doi.org/10.1021/es1013714>
- Gui, Q., Fu, L., Hu, Y., Di, H., Liang, M., Wang, S., Zhang, L., Dong, E., (2023). Oxidative pretreatment of refractory gold ore using persulfate under ultrasound for efficient leaching of gold by a novel eco-friendly

- lixiviant: Demonstration of the effect of particle size and economic benefits. *Hydrometallurgy* 221. <https://doi.org/10.1016/j.hydromet.2023.106110>
- Hao, F., Guo, W., Wang, A., Leng, Y., Li, H., (2014). Intensification of sonochemical degradation of ammonium perfluorooctanoate by persulfate oxidant. *Ultrason Sonochem* 21, 554–558. <https://doi.org/10.1016/j.ultsonch.2013.09.016>
- Hao, J., Wang, X., Wang, Y., Wu, Y., & Guo, F. (2022). Optimizing the Leaching Parameters and Studying the Kinetics of Copper Recovery from Waste Printed Circuit Boards. *ACS Omega*, 7(4), 3689–3699. <https://doi.org/10.1021/acsomega.1c06173>
- Holmes, P. R., & Crundwell, F. K. (2000). The kinetics of the oxidation of pyrite by ferric ions and dissolved oxygen: An electrochemical study. *Geochimica et Cosmochimica Acta*, 64(2), 263-274. [https://doi.org/10.1016/S0016-7037\(99\)00296-3](https://doi.org/10.1016/S0016-7037(99)00296-3)
- House, D.A., (1962). Kinetics and Mechanism of Oxidations by Peroxydisulfate. *Chem Rev* 62, 185–203. <https://doi.org/https://doi.org/10.1021/cr60217a001>
- Huang, Y., Jia, Z., Wang, W., Yao, J., Gao, R., Xu, L., Zhang, H., Zhang, Y., & Song, X. (2023). Study on Electrochemical Behavior of Oxidized Pyrite in Alkaline Electrolyte. *Minerals*, 13(8). <https://doi.org/10.3390/min13081070>
- Iraola-Arregui, I., Van Der Gryp, P., & Görgens, J. F. (2018). A review on the demineralisation of pre- and post-pyrolysis biomass and tyre wastes. In *Waste Management* (Vol. 79, pp. 667–688). Elsevier Ltd. <https://doi.org/10.1016/j.wasman.2018.08.034>
- Irum, S., Akhtar, J., Sheikh, N., Munir, S., (2017). Oxidative desulfurization of Chakwal coal using potassium permanganate, ferric sulfate, and sodium hypochlorite. *Energy Sources, Part A: Recovery, Utilization and Environmental Effects* 39, 426–432. <https://doi.org/10.1080/15567036.2016.1222028>
- Jefferson, M., Yenial-Arslan, U., Evans, C., Curtis-Morar, C., O'Donnell, R., Parbhakar-Fox, A., & Forbes, E. (2023). Effect of pyrite textures and composition on flotation performance: A review. In *Minerals Engineering* (Vol. 201). Elsevier Ltd. <https://doi.org/10.1016/j.mineng.2023.108234>
- Johnson, D.B., Hallberg, K.B., (2005). Acid mine drainage remediation options: A review. *Science of the Total Environment* 338, 3–14. <https://doi.org/10.1016/j.scitotenv.2004.09.002>
- Karim, A. V., Jiao, Y., Zhou, M., Nidheesh, P. V., (2021). Iron-based persulfate activation process for environmental decontamination in water and soil. *Chemosphere*. <https://doi.org/10.1016/j.chemosphere.2020.129057>
- Karppinen, A., Seisko, S., & Lundström, M. (2024). Atmospheric leaching of Ni, Co, Cu, and Zn from sulfide tailings using various oxidants. *Minerals Engineering*, 207. <https://doi.org/10.1016/j.mineng.2024.108576>
- Khataee, A., Gholami, P., Sheydaei, M., Khorram, S., Joo, S.W., (2016). Preparation of nanostructured pyrite with N₂ glow discharge plasma and the study of its catalytic performance in the heterogeneous Fenton process. *New Journal of Chemistry* 40, 5221–5230. <https://doi.org/10.1039/c5nj03594e>
- La Brooy, S., Linge, H., & Walker, G. (1994). Review of gold extraction from ores. *Minerals Engineering*, 7(10), 1213-1241. [https://doi.org/10.1016/0892-6875\(94\)90114-7](https://doi.org/10.1016/0892-6875(94)90114-7)
- Levakov, I., Han, J., Ronen, Z., & Dahan, O. (2021). Inhibition of perchlorate biodegradation by ferric and ferrous iron. *Journal of Hazardous Materials*, 410. <https://doi.org/10.1016/j.jhazmat.2020.124555>
- Liang, C., Wang, Z.S., Bruell, C.J., (2007). Influence of pH on persulfate oxidation of TCE at ambient temperatures. *Chemosphere* 66, 106–113. <https://doi.org/10.1016/j.chemosphere.2006.05.026>
- Li, J., Lu, J., Lu, X., Tu, B., Ouyang, B., Han, X., & Wang, R. (2016). Sulfur Transformation in Microbially Mediated Pyrite Oxidation by *Acidithiobacillus ferrooxidans*: Insights From X-ray Photoelectron Spectroscopy-Based Quantitative Depth Profiling. *Geomicrobiology Journal*, 33(2), 118–134. <https://doi.org/10.1080/01490451.2015.1041182>
- Li, X., Jie, B., Lin, H., Deng, Z., Qian, J., Yang, Y., Zhang, X., (2022). Application of sulfate radicals-based advanced oxidation technology in degradation of trace organic contaminants (TrOCs): Recent advances and prospects. *J Environ Manage* 308. <https://doi.org/10.1016/j.jenvman.2022.114664>
- Liu, C., Liu, Y., Zeng, S., & Li, D. (2023). Investigating the oxidation mechanism of facet-dependent pyrite: implications for the environment and sulfur evolution. *Environ. Sci.: Processes Impacts*, 25(12), 2031–2041. <https://doi.org/10.1039/D3EM00221G>
- Luo, C., Jiang, J., Ma, J., Pang, S., Liu, Y., Song, Y., Guan, C., Li, J., Jin, Y., Wu, D., (2016). Oxidation of the odorous compound 2,4,6-trichloroanisole by UV activated persulfate: Kinetics, products, and pathways. *Water Res* 96, 12–21. <https://doi.org/10.1016/j.watres.2016.03.039>
- Marsden, J., House, C.Iain., (2006). *Chemistry of Gold Extraction*. Ellis Horwood Ltd.
- Marzocco, C.J., (1999). The Enthalpy of Decomposition of Hydrogen Peroxide: A General Chemistry Calorimetry Experiment. *J Chem Educ* 76, 1517. <https://doi.org/10.1021/ed076p1517>
- Matzek, L.W., Carter, K.E., (2016). Activated persulfate for organic chemical degradation: A review. *Chemosphere* 151, 178–188. <https://doi.org/10.1016/j.chemosphere.2016.02.055>

- Miller, P., Brown, A.R.G., (2016). Bacterial Oxidation of Refractory Gold Concentrates, in: *Gold Ore Processing: Project Development and Operations*. Elsevier, pp. 359–372. <https://doi.org/10.1016/B978-0-444-63658-4.00022-0>
- Mitra, K., Moreland, E. L., & Catalano, J. G. (2020). Capacity of chlorate to oxidize ferrous iron: Implications for iron oxide formation on mars. *Minerals*, 10(9), 1–19. <https://doi.org/10.3390/min10090729>
- Nicol, M. J. (2020). The role and use of hydrogen peroxide as an oxidant in the leaching of minerals. 1. acid solutions. *Hydrometallurgy*, 193. <https://doi.org/10.1016/j.hydromet.2020.105328>
- Petrović, S. J., Bogdanović, G. D., Antonijević, M. M., Vukčević, M., & Kovačević, R. (2023). The Extraction of Copper from Chalcopyrite Concentrate with Hydrogen Peroxide in Sulfuric Acid Solution. *Metals*, 13(11). <https://doi.org/10.3390/met13111818>
- Peyton, G. R. (1993). The free-radical chemistry of persulfate-based total organic carbon analyzers. *Marine Chemistry*, 41(1-3), 91-103. [https://doi.org/10.1016/0304-4203\(93\)90108-Z](https://doi.org/10.1016/0304-4203(93)90108-Z)
- Pokrovski, G. S., Kokh, M. A., Proux, O., Hazemann, J. L., Bazarkina, E. F., Testemale, D., Escoda, C., Boiron, M. C., Blanchard, M., Aigouy, T., Gouy, S., de Parseval, P., & Thibaut, M. (2019). The nature and partitioning of invisible gold in the pyrite-fluid system. *Ore Geology Reviews*, 109, 545–563. <https://doi.org/10.1016/j.oregeorev.2019.04.024>
- Pourbaix, M., (1974). *Atlas of electrochemical equilibria in aqueous solutions*, 2d English. ed. National Association of Corrosion Engineers, Houston, Texas.
- Radha, A. V., Lander, L., Rouse, G., Tarascon, J.M., Navrotsky, A., (2015). Thermodynamic stability and correlation with synthesis conditions, structure and phase transformations in orthorhombic and monoclinic $\text{Li}_2\text{M}(\text{SO}_4)_2$ (M = Mn, Fe, Co, Ni) polymorphs. *J Mater Chem A Mater* 3, 2601–2608. <https://doi.org/10.1039/c4ta05066e>
- Rodríguez-Rodríguez, C., Nava-Alonso, F., & Uribe-Salas, A. (2018). Arsenopyrite Oxidation with Ozone: Stoichiometry and Kinetics. *Ozone: Science and Engineering*, 40(4), 284–292. <https://doi.org/10.1080/01919512.2017.1417113>
- Rogozhnikov, D., Karimov, K., Shoppert, A., Dizer, O., & Naboichenko, S. (2021). Kinetics and mechanism of arsenopyrite leaching in nitric acid solutions in the presence of pyrite and Fe(III) ions. *Hydrometallurgy*, 199. <https://doi.org/10.1016/j.hydromet.2020.105525>
- Salas-Martell, D., Pareja-Guzman, G., Tello-Hijar, J., Rodriguez-Reyes, J.C.F., (2020). Leaching of a pyrite-based ore containing copper using sulfuric acid and hydrogen peroxide. *International Journal of Industrial Chemistry* 11, 195–201. <https://doi.org/10.1007/s40090-020-00212-2>
- Spietz, R. L., Payne, D., Kulkarni, G., Metcalf, W. W., Roden, E. E., & Boyd, E. S. (2022). Investigating Abiotic and Biotic Mechanisms of Pyrite Reduction. *Frontiers in Microbiology*, 13. <https://doi.org/10.3389/fmicb.2022.878387>
- Tehrani, M. E. H. N., Naderi, H., & Rashchi, F. (2021). Electrochemical study and XPS analysis of chalcopyrite dissolution in sulfuric acid in the presence of ethylene glycol. *Electrochimica Acta*, 369. <https://doi.org/10.1016/j.electacta.2020.137663>
- Tu, Z., Guo, C., Zhang, T., Lu, G., Wan, J., Liao, C., & Dang, Z. (2017). Investigation of intermediate sulfur species during pyrite oxidation in the presence and absence of *Acidithiobacillus ferrooxidans*. *Hydrometallurgy*, 167, 58–65. <https://doi.org/10.1016/j.hydromet.2016.11.001>
- Urbansky, E.T., (2002). Perchlorate as an Environmental Contaminant. *Environmental Science and Pollution Research* 9, 187–192. <https://doi.org/10.1065/espr2002.05.117>
- Xie, J., Yang, C., Li, X., Wu, S., Lin, Y., (2023). Generation and engineering applications of sulfate radicals in environmental remediation. *Chemosphere* 339. <https://doi.org/10.1016/j.chemosphere.2023.139659>
- Xu, G., Deng, F., Fan, W., Shi, Z., Ma, R., & Wang, C. (2022). Pre-oxidation of refractory gold concentrate by electrochemical methods in alkaline electrolyte. *Materials Today Communications*, 31. <https://doi.org/10.1016/j.mtcomm.2022.103397>
- Yadav, V.K., Ali, D., Khan, S.H., Gnanamoorthy, G., Choudhary, N., Yadav, K.K., Thai, V.N., Hussain, S.A., Manhrdas, S., (2020). Synthesis and characterization of amorphous iron oxide nanoparticles by the sonochemical method and their application for the remediation of heavy metals from wastewater. *Nanomaterials* 10, 1–17. <https://doi.org/10.3390/nano10081551>
- Zhang, F., Xi, L., Zhao, M., Du, Y., Ma, L., Chen, S., Ye, H., Du, D., & Zhang, T. C. (2022). Efficient removal of Cr(VI) from aqueous solutions by polypyrrole/natural pyrite composites. *Journal of Molecular Liquids*, 365. <https://doi.org/10.1016/j.molliq.2022.120041>
- Zhong, S.P., (2015). Leaching kinetics of gold bearing pyrite in $\text{H}_2\text{SO}_4\text{-Fe}_2(\text{SO}_4)_3$ system. *Transactions of Nonferrous Metals Society of China (English Edition)* 25, 3461–3466. [https://doi.org/10.1016/S1003-6326\(15\)63983-8](https://doi.org/10.1016/S1003-6326(15)63983-8)